IMTC 2005 – Instrumentation and Measurement
Technology Conference
Ottawa, Canada, 17-19 May 2005

Energy Scavenging for Inductively Coupled Passive RFID Systems

Bing Jiang[1], Joshua R. Smith[2], Matthai Philipose[2], Sumit Roy[1],
Kishore Sundara-Rajan[1,2], and Alexander V. Mamishev[1]
[1]Department of Electrical Engineering, University of Washington, Seattle, WA 98195
[2] Intel Research, Seattle, WA 98105

Abstract *– Deployment of passive RFID systems or RFID-enhanced sensor networks requires good understanding of the energy scavenging principles. This paper focuses on the energy scavenging design considerations of inductively coupled passive RFID systems. The theoretical estimation of the power by an RF antenna is derived, and the effect of the design parameters on the harvested power is investigated. It is shown that the power delivery performance is largely affected by the tag load at the reader. An adaptive matching circuit at the reader is proposed for achieving optimum power delivery performance when the reader has a variable load. Experimental studies confirm analytical derivations.*

Keywords *– RFID, passive tag, antenna design, inductive antenna, impedance match, energy scavenging, power harvesting.*

I. INTRODUCTION

The Radio-Frequency Identification (RFID) technology is of growing interest to commerce, industry, and academia. This technology can be used not only for identification, but also for tracking objects in a supply chain, monitoring the object's status, enhancing security, and as well as many other applications [1].

The RFID system consists of readers/interrogators, tags/transponders, and an information managing host computer [2]. Tags can be categorized as: (a) active tag, which has a battery that supplies power to all functions; (b) semi-passive tag, which has a battery used only to power the tag IC, and not for communication; (c) passive tag, which has no battery on it. The absence of a power supply makes passive tags much cheaper and of much greater longevity than active tags. This paper focuses on the 13.56 MHz inductive passive RFID system, one of the mainstream RFID products, since this frequency is better able to penetrate non-metal substrates than UHF and microwave bands due its longer wavelength.

As a low-cost wireless communication platform, the passive RFID system provides a possibility of implementing wireless sensor networks through integration of the RFID tag ICs and MEMS sensors, as shown in Fig. 1. This proposed system is called here "the enhanced RFID system." Such a system will not work well unless the enhanced tag receives enough energy from the reader. Successful energy scavenging in passive RFID systems will help extending their applications.

Passive tags obtain impinging energy during reader interrogation periods, and this energy is used to power tag IC. For the maximum reading range, one has to ensure the maximum power transfer efficiency from the reader to the tag. What makes the problem challenging is that in the case of inductively coupled reader-tag, the reader must deal with a changing effective load due to (a) the location-dependent mutual coupling effect between the reader and tag and (b) unpredictable number of tags in the read zone of the reader.

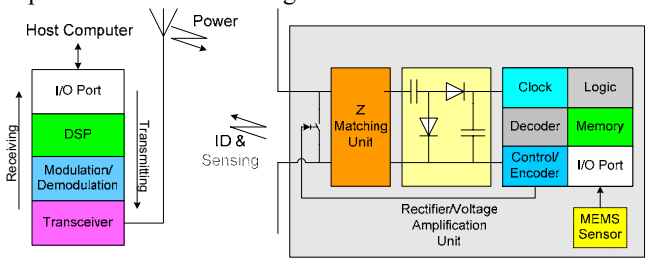

Fig. 1. The RFID reader-tag (sensing node) system

This paper presents a study of how mutual inductance between the reader and the tag affects the amount of power generated at the tag. The mutual inductance can be viewed as a variable load at the reader. This load may lead to mismatch and poor power transfer efficiency if a fixed reader impedance matching circuit is implemented; accordingly, an adaptive impedance matching network at the reader is proposed. The antenna design guidelines to improve the power transfer from the reader to the tags are given.

II. BACKGROUND

A. L-match network

Impedance matching is necessary in the design of RF circuitry in order to provide maximum power delivery between a source and its load and improve the signal to noise ratio of the system. Generally, an L, T or π-matching network can be used to match the load to the source [3]. In this paper, the L-matching network is used due to its simplicity and ease of tuning. Fig. 2 shows the lumped circuits of the loop antenna only (left) and the loop antenna with the L-match network (right), where X_1 and X_2 are reactive elements for the matching purpose, and R_{ANT} and L_{ANT} are the resistance and self-inductance of the antenna.

The configuration in Fig. 2 transforms a larger impedance to a smaller value with the real part equal to source resistance R_{sr}. Fig. 2 is valid only when $|R_{ANT} + j\omega L_{ANT}| > R_{sr}$ [4]. Thus, the impedance of an inductive antenna is matched to the source impedance as

$$jX_2 + \frac{(R_{ANT} + j\omega L_{ANT})\, jX_1}{R_{ANT} + j\omega L_{ANT} + jX_1} = R_{sr} \tag{1}$$

where ω is the angular frequency. R_{ANT} in (1) can be expressed as

$$R_{ANT} \approx \frac{l}{2w}\sqrt{\frac{\pi f \mu}{\sigma}} \tag{2}$$

where σ and μ are the conductor's electrical conductivity and magnetic permeability; l is the length of the loop; w is the trace width; and f is the signal frequency [5].

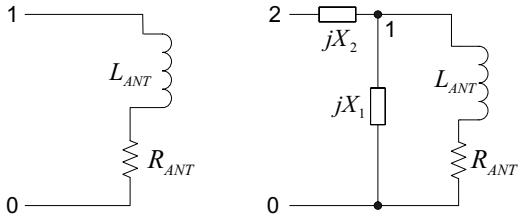

Fig. 2. L-matching network (left: original antenna; right: matched antenna).

It is difficult to estimate accurately L_{ANT} in (1), especially for a planar coil. For a round planar spiral coil L_{ANT} can be roughly approximated by (3) with at least 80% accuracy

$$L_{ANT} \approx 31.33\mu N^2 \frac{a^2}{8a + 11c} \tag{3}$$

where N is the number of turns in the loop; a is the coil mean radius; and c is the thickness of the winding [6]. Analytical expressions for planar rectangular coils are available in [7]. Their accurate values can be approximated with numerical simulation software, such as Sonnet®. When the resistance and inductance of the loop are determined, X_1 and X_2 can be solved using (1).

B. Induced Magnetic Field

A changing current along a conductor induces a changing magnetic field. When another conductor is placed in this field, an induced voltage is generated. In order to simplify the calculation of the magnetic field, the inductive loop can be treated as a series of small dipoles. Fig. 3 shows a dipole model. The magnetic field in the vicinity of the inductor is

$$\boldsymbol{B} \approx \frac{\mu I_0}{2\pi} e^{j\omega t} \frac{h}{r\sqrt{r^2 + h^2}} \tag{4}$$

where h is the half-length of the dipole, I_0 is the amplitude of the current along the loop, μ is the permeability of air, and s is the distance from P to the center of the dipole [8].

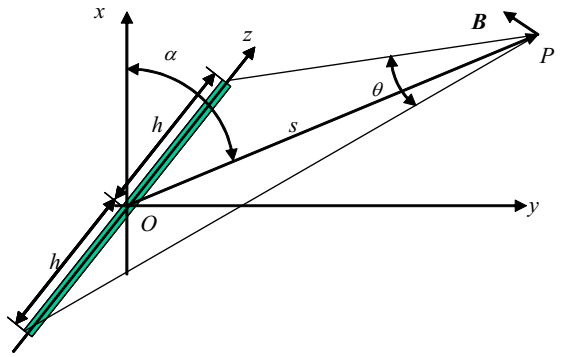

Fig. 3. Magnetic field generated by a dipole.

Based on (4), the magnetic field along the central axis x generated by a rectangular inductive loop antenna can be expressed as

$$B_x = KI_0 \tag{5}$$

$$K \approx \frac{\mu}{\pi}\sum_{i=1}^{n_r} \frac{a_i b_i}{\sqrt{a_i^2 + b_i^2 + x^2}}\left(\frac{1}{a_i^2 + x^2} + \frac{1}{b_i^2 + x^2}\right) \tag{6}$$

where B_x is the amplitude of the magnetic field component along the x axis, a_i and b_i are the half side-length of the rectangular loop, and n_r is the number of turns.

C. Induced Voltage

When a loop is placed in the magnetic field, an induced voltage is generated, and is calculated as

$$V_t = \int_C \boldsymbol{E} \cdot d\boldsymbol{l} = -\frac{\partial}{\partial t}\int_S \boldsymbol{B} \cdot d\boldsymbol{s} \tag{7}$$

where C is the length of the loop curve, S is the area of the loop, $\boldsymbol{E}$ is the electric field vector, $\boldsymbol{l}$ is the tangent direction of the loop curve, and $\boldsymbol{s}$ is the normal direction of the loop surface. Since the RFID tag is usually very small, $\boldsymbol{B}$ is treated as a constant at the tag location. Because the induced voltage from each turn is serially connected, for a tag with a n_t turn antenna the induced voltage is

$$V_t \approx -j\omega B\sum_{i=1}^{n_t} S_i = -j\omega I_0 K\sum_{i=1}^{n_t} S_i \tag{8}$$

Equation (8) shows that V_t can be varied value by adjusting the design parameters, such as the number of turns and the dimension of the loop with I_0 is treated as a constant. This approximation is based on the assumption that the magnetic field generated by the tag in the direction opposite to the magnetic field generated by the reader is negligible. This assumption is usually true when the reader antenna and

the tag antenna are far away from each other. However, this assumption cannot be used to predict the situation when the tag is working in the near field of the reader antenna, since I_0 is forced to change in this case. In order to reach optimum power delivery performance, the accurate estimations of I_0 and V_t are presented below.

III. LOADING EFFECT

The induced voltage on the tag generates current along the tag loop antenna, which generates an EM field in the direction opposite to the triggering EM field. The reader antenna and the tag antenna can be treated as a pair of weakly coupled transformers, as shown in Fig. 4 with a coupling factor M [9]. Therefore, the induced voltage at the tag can also be derived as

$$V_t = j\omega M I_0 \tag{9}$$

According to (8), the coupling coefficient is determined as

$$M = -K\sum_{i=1}^{n_t} S_i \tag{10}$$

Equation (10) shows that M is only determined by the geometry and the relative position of the two antennas.

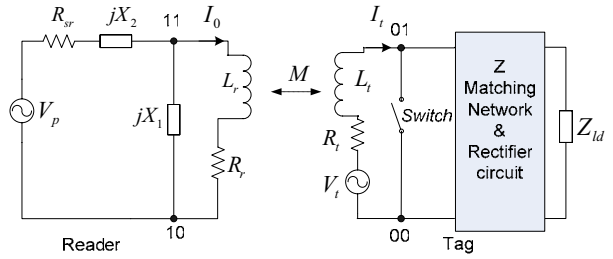

Fig. 4. The circuit schematics of the coupled RFID reader antenna and tag antenna.

Based on the KVL and KCL, the following equations are derived for a RFID reader antenna when it is loading tags and is matched with an L-matching network:

$$\begin{cases} V_p = R_{sr} I + Z_2 I + V_r \\ I = I_0 + \dfrac{V_r}{Z_1} \\ V_r = \left(R_r + j\omega L_r\right) I_0 + j\omega M I_t \end{cases} \tag{11}$$

where R_{sr} is the source resistance; R_r and L_r are the resistance and inductance of the reader antenna, respectively; V_p and V_r are the driving source voltage and voltage at the reader antenna, respectively; I, I_0, and I_t are the current flowing through R_{sr}, the reader antenna, and the tag antenna, respectively; and $Z_1 = jX_1$ and $Z_2 = jX_2$ are the impedances of the LC matching elements.

Using KVL for the tag circuit yields

$$j\omega M I_0 + \left(R_t + j\omega L_t\right) I_t + Z_t I_t = 0 \tag{12}$$

where R_t, L_t, are the tag resistance and inductance, and Z_t is the tag impedance at the port 00-01, including the matching network, rectifier, and load impedance Z_{ld}, as shown in Fig. 4.

The induced power on the tag is rectified and fed to the load. Fig. 5 shows the rectifier circuit. The detailed discussion on the rectifier design can be found in [10,11].

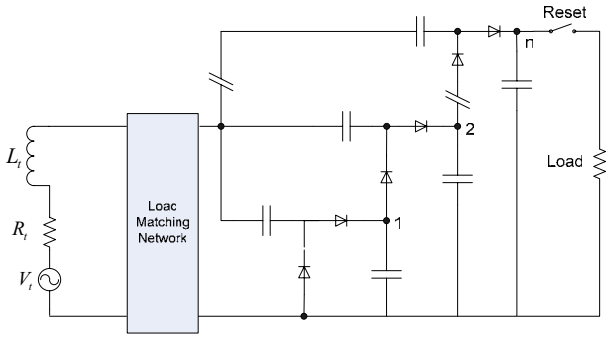

Fig. 5. The lumped circuit model for the rectifier circuit.

If the power loss due to the rectifier circuit is negligible, the maximum output power can be reached when the load impedance is matched to the source impedance, i.e.,

$$Z_t = R_t - j\omega L_t \tag{13}$$

Therefore, the current I_t is given by

$$I_t = -\frac{1}{2R_t} j\omega M I_0 \tag{14}$$

Replacing I_t in (11) by using (14), I_0 is solved as

$$\left(1+\left(\frac{2R_{sr}\left(R_r + j\omega L_r + Z_1\right) + Z_1^2}{2R_{sr}\left(R_r + j\omega L_r + Z_1\right)^2}\right)\frac{\left(\omega M\right)^2}{2R_t}\right) I_0 = \frac{Z_1}{R_r + j\omega L_r + Z_1}\frac{V_p}{2R_{sr}} \tag{15}$$

I_0 is still unsolved, since L_r and Z_1 remain unknown. When the unloaded loop antenna ($M = 0$) is matched to the source resistance R_{sr}, the power dissipated by the antenna is

$$P_{ANT} = \frac{1}{2}\left(\frac{1}{2}\frac{V_p^2}{2R_{sr}}\right) = \frac{V_p^2}{8R_{sr}} \tag{16}$$

Since the LC elements do not dissipate power, the power P_{ANT} is the power dissipated by R_r, i.e.,

$$\left|I_0\right|_{unload} = \frac{V_p}{2R_{sr}}\sqrt{\frac{R_{sr}}{R_r}} \tag{17}$$

When $M = 0$, I_0 can also be derived from (11) as

$$I_0 = \frac{V_p}{2R_{sr}}\frac{Z_1}{R_r + j\omega L_r + Z_1} \tag{18}$$

As a result,

$$\frac{Z_1}{R_r + j\omega L_r + Z_1} = \sqrt{\frac{R_{sr}}{R_r}} e^{j\vartheta} \tag{19}$$

where ϑ is the phase.

Introducing (19) into (15), (15) is rewritten as

$$\left(1+\left(\omega C_1\sqrt{\frac{R_{sr}}{R_r}}e^{j(\vartheta+\pi/2)}+\frac{1}{2R_r}e^{j2\vartheta}\right)\frac{(\omega M)^2}{2R_t}\right)I_0=\sqrt{\frac{R_{sr}}{R_r}}e^{j\vartheta}\frac{V_p}{2R_{sr}} \quad (20)$$

The values of ωC_1 and ϑ in (20) are usually very small, therefore (20) is further simplified as follows

$$I_0\approx\sqrt{\frac{R_{sr}}{R_r}}\frac{V_p}{2R_{sr}}\left(1+\frac{1}{4}\frac{(\omega M)^2}{R_rR_t}\right)^{-1} \quad (21)$$

Based on (16) the harvested power P_T on the RFID tag IC circuitry is

$$P_T=\frac{1}{8R_t}|\omega MI_0|^2 \quad (22)$$

IV. DISCUSSION

A. Small Load Effect

When $(\omega M)^2/(4R_rR_t)<<1$,

$$P_T\approx\frac{1}{32R_tR_rR_{sr}}(\omega V_p)^2|M|^2 \quad (23)$$

Equation (10) and (6) also show that $|M|\propto 1/r$ in the near field, but $|M|\propto 1/r^2$ in the far field. This relationship indicates that the inductive RFID tags can only work in the near field of the reader antenna with a limited range. For a tag located in the center of the square antenna and based on (2) and (3),

$$P_T=\frac{f\mu}{256\pi R_{sr}}V_p^2\frac{1}{h_r^3}\sigma w_r w_t n_r n_t h_t \quad (24)$$

where w_r and w_t are the trace width of the reader antenna and the tag antenna, h_r and h_t are the half side length of the reader antenna and the tag antenna, and σ and μ are the conductivity and magnetic permeability of the conductor. Equation (24) explicitly expresses the effect of design parameters on P_T.

Usually, an expected working range is pre-specified as one of the design goals; therefore, the determination on the antenna size is important in the design procedure. For a square loop, (9) can be rewritten as

$$V_t=k_0\frac{h^2}{(x^2+h^2)\sqrt{x^2+2h^2}} \quad (25)$$

where k_0 is a constant, and x is the expected range. By letting $dV_t/dh=0$, we can obtain the optimum half side length of the loop

$$h=\frac{1}{2}\left(1+\sqrt{5}\right)d \quad (26)$$

For a circular loop, the dipole can be approximated as

$$h\approx r\frac{\Delta\theta}{2} \quad (27)$$

where r is the radium of the circular loop, and θ is the sector angle to the cord $2h$, as shown in Fig. 3. B_x is integrated as

$$B_x=\int_0^{2\pi}\frac{r^2}{2\left(d^2+r^2\right)^{3/2}}d\theta=\frac{\pi r^2}{\left(d^2+r^2\right)^{3/2}} \quad (28)$$

and,

$$V_t=k_0\pi r^2\left(d^2+r^2\right)^{-3/2} \quad (29)$$

By letting $dV_t/dr=0$, we can obtain the optimum radius of the loop

$$r=\sqrt{2}d \quad (30)$$

B. Large Load Effect

When $(\omega M)^2/(4R_rR_t)>1$,

$$P_T\approx V_p^2\frac{R_tR_r}{2|\omega M|^2R_{sr}} \quad (31)$$

i.e., P_T decreases with the increase of the coupling factor $|M|$, because larger coupling results in a smaller I_0, and, consequently, a lesser delivered power. There are two possible situations that may result in large coupling: (a) many tags in the reader operating range; (b) a closely located tag. When a tag is moved closely to the reader, the output voltage may increase gradually until it reaches its peak, and after that it drops. In other words, a relatively large coupling effect could lower the power transfer between the reader and the tag. Simulations illustrating this effect are as shown in Fig. 6.

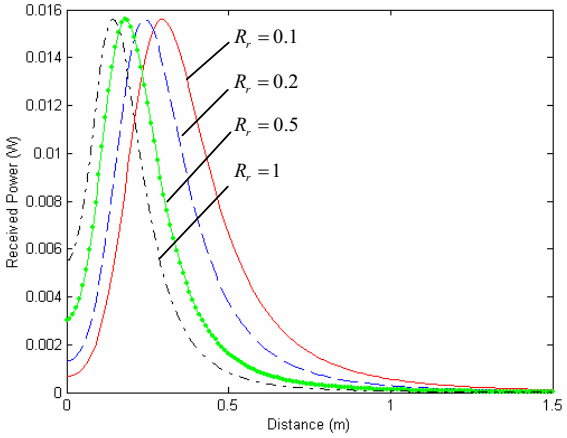

Fig. 6. The demonstrated relationship between the received power and coupling factor, which is simulated with a reader antenna with S=20cm*20cm and one turn, a tag with S=0.023m^2 (10 turns) and R_t =6.2 Ω, V_p =5, and R_{sr} =50 Ω.

In order to improve poor power transfer efficiency, an adaptive matching network that changes the reactive element values to match the changing load may be used [12,13]. However, it is difficult to implement the adaptive matching due to the lack of feedback loop. Fig. 7 shows that a modified matching circuit is used on the RFID reader antenna. The only drawback of this method is that the tag takes longer time to respond the reader inquiry, since the reader needs more time to sweep different configurations. Fig. 8 shows the power delivery improvement over the fixed matching circuit.

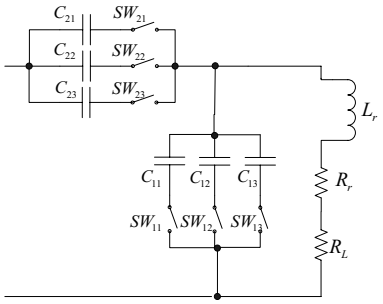

Fig. 7. The schematics of the adaptive L-match network.

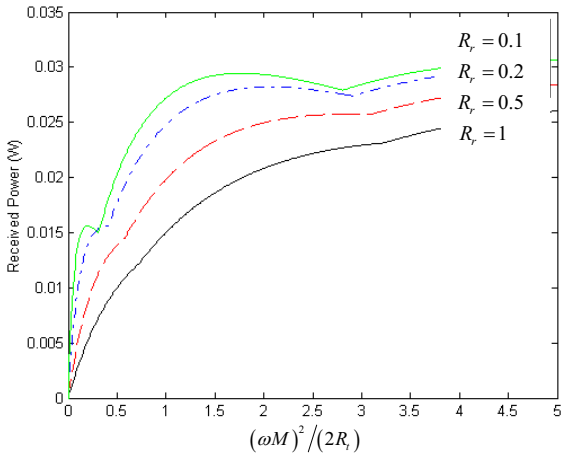

Fig. 8. The simulated result by using the adaptive L-match network.

Based on the maximum power transfer with impedance matching, the received power by the tag by using the fixed matching algorithms has the maximum value that is 12.5% of the total consumed power $V_p^2(8R_{sr})^{-1}$. However, the maximum power efficiency for the complete adaptive matching network is improved by 25% as shown in Fig. 8.

V. EXPERIMENTAL RESULTS

A tag with a loop antenna was designed for testing with the following specifications: 15-turns, 46×46 mil^2 outer dimensions, 0.254 mm gap, and 0.254 mm track width. A voltage doubler is used to raise the output voltage. Experiments have been performed to evaluate the effect of design parameters. Fig. 9, Fig. 10, and Fig. 11 show experimental results with V_p=3 V, where x axis is the distance between the center of reader antenna and the center of tag antenna, and y axis is the output voltage generated on the tag.

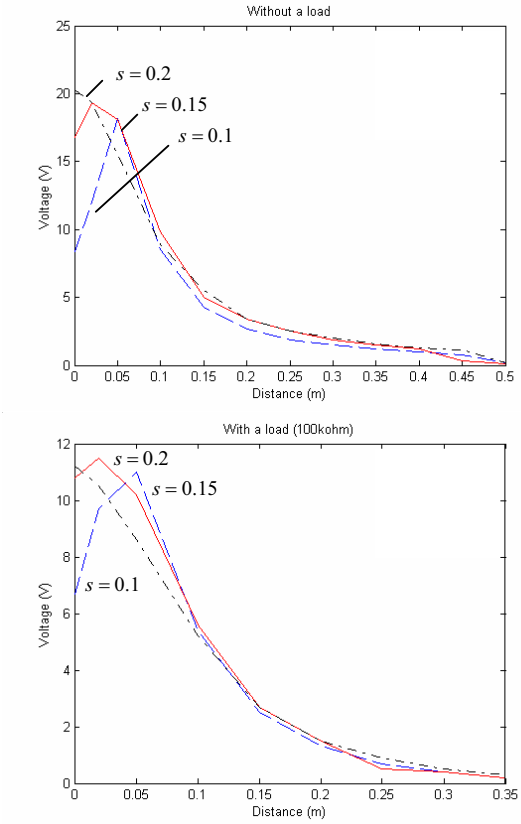

Fig. 9. The characteristics of inductive coupling in RFID systems (s—the side length of RFID reader antenna)

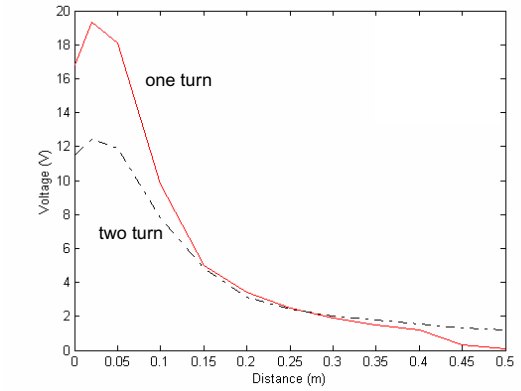

Fig. 10. The characteristics of inductive coupling in RFID systems –turn effect (the side length of reader antenna is 10cm).

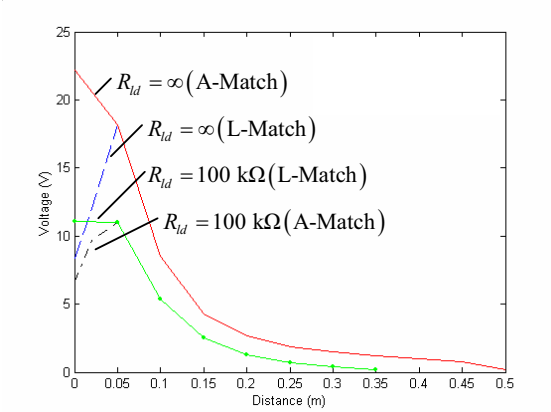

Fig. 11. The characteristics of inductive coupling in RFID systems –load effect (the side length of reader antenna is 10cm).

The voltage generated in the tag drops as the load on it increases. This effect is highly pronounced when the distance between the tag and reader is small. The fall in the voltage is caused by changes in the coupling coefficient between the two antennae. By using an adaptive matching circuit, the coupling coefficient can be changed to optimize power transfer with varying load. Fig. 11 shows the voltage generated as a function of distance between the tag and the reader at two different load levels for a fixed impedance matching circuit, and an adaptive matching circuit. It can be seen that the adaptive matching circuit offers a significant improvement over the fixed circuit.

VI. EFFECT OF ENVIRONMENT

The above discussion is based on the assumption that the loop antennas are surrounded by the air. Actually, it is possible that antennas are placed on the top of a metal frame, which may result in a different magnetic field distribution.

Let us assume the antenna loop has a distance d to a metal frame. The image of the antenna loop under the frame plane has the exact distance d to the metal plane. Fig. 12 shows the configuration.

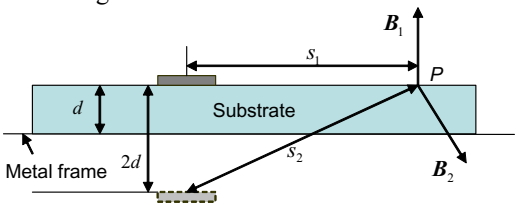

Fig. 12. The calculation model for the magnetic field of an antenna loop with a metal substrate.

Since $B_x = B_{1x} + \cos(\delta) B_{2x}$, B_x is rewritten as

$$B_x = \frac{\sqrt{2}\mu I_0}{4\pi} e^{j\omega t}\left(s^{-1} + \cos(\delta)\, s\left(s^2 + (2d)^2\right)^{-1}\right) \qquad (32)$$

where $\cos(\delta) = -1$ if the dipole is perfectly parallel to the metal plane [4]. When d is small compared to s, the above equation is simplified as

$$B_x = \frac{1}{4\pi}\sqrt{2}\mu I_0 e^{j\omega t}(2d)^2 s^{-3} = \frac{1}{\pi}\sqrt{2}\mu I_0 d^2 s^{-3} e^{j\omega t} \qquad (33)$$

It shows that the magnetic field $\boldsymbol{B}$ decreases a lot due to the metal frame. In order to reduce this effect, the loop antenna should be kept a distance away from the metal frame, and a loop with a smaller size is preferred when it is possible. As a result, the matching elements should be correspondingly adjusted to reach optimum power delivery performance.

VII. CONCLUSIONS

An analytical method to compute the power delivered to the RFID tag as a function of the mutual inductance between the antennae of the tag and reader was introduced. The effect of the variable mutual coupling on the power delivery was discussed. An adaptive impedance matching circuit was proposed as a solution to mitigate the detrimental effect of the load on the power transfer efficiency. The design procedure of a power harvesting circuit for antenna specifications was also outlined, including the loop size.

REFERENCES

[1] V. Stanford, "Pervasive Computing Goes the Last Hundred Feet With RFID Systems," *IEEE Pervasive Computing*, vol. 2, no. 2, pp. 9-14, 2003.

[2] K. Finkenzeller, *RFID handbook: fundamentals and applications in contactless smart cards and identification,* 2 ed., Wiley, 2003.

[3] C. Bowick, *RF circuit design,* Newnes, 1997.

[4] D. Pozar, *Microwave engineering,* 2 ed., John Wiley & Sons, 2003.

[5] "AN831: Matching small loop antennas to rfPIC devices," Microchip application notes. 2002.

[6] "Simple Inductance Formulas for Radio Coils," *Proceedings of the IRE*, vol. 16, no. 10, 1928.

[7] H. Greenhouse, "Design of Planar Rectangular Microelectronic Inductors," *IEEE Transactions on Parts, Hybrids, and Packaging*, vol. 10, no. 2, pp. 101-109, 1974.

[8] J. Kraus, *Antennas,* 2 ed., McGraw-Hill, 1988.

[9] "AN680: microID 13.56 MHz RFID system design guide," Microchip application notes. 2001.

[10] Z. Zhu, B. Jamali, and P. H. Cole, "Brief comparison of different rectifier structures for HF and UHF RFID (Phase II)," Auto-ID Labs, 2004.

[11] Z. Zhu, B. Jamali, and P. H. Cole, "Brief comparison of different rectifier structures for HF and UHF RFID (Phase I)," Auto-ID Labs, 2004.

[12] B. Nauta and M. B. Dijkstra, "Analog Line Driver With Adaptive Impedance Matching," *IEEE Journal of Solid-State Circuits*, vol. 33, no. 12, pp. 1992-1998, 1998.

[13] M. Thompson and J. K. Fidler, "Application of the Genetic Algorithm and Simulated Annealing to LC Filter Tuning," *IEE Proceedings G- Circuits, Devices and Systems*, vol. 48, no. 4, pp. 177-182, 2001.